A MULTIMODE SMALL SIGNAL ANALYSIS OF THE SINGLE PASS FREE ELECTRON LASER

G. DATTOLI, A. MARINO and A. RENIERI

Comitato Nazionale Energia Nucleare, Centro di Frascati, C.P. 65 - 00044 Frascati, Rome, Italy

Received 23 July 1980

We analyze the small signal multimode aspects of the single pass free electron laser and study the operating conditions and the relevant laser parameters.

During the last times, the problem of theoretically understanding the free electron laser (FEL) [1] behaviour has been widely considered.

In particular two of the present authors (G.D. and A.R.) firstly analysed the FEL theory in the multimode regime [2], and applied the small signal multimode analysis to the FEL Storage Ring Operation [3].

The aim of the present paper is twofold

(a) to perform a first step towards the interpretation of the single pass machine FEL behaviour [1], by analyzing the small signal multimode aspects and studying the main features of the laser parameters such as gain, spectrum bandwidth and so on;

(b) to understand the rise-time of the laser pulse and the operating conditions suitable to have a laser action.

In developing the analysis we shall employ the main results of refs. [2,3], where the essential features of the multimode small signal theory have been carried out.

In the second of refs. [2] the laser modes evolution equations have been written down and read (for circularly polarized laser field)

$$\Delta W_i = -W_i\gamma_T - A(1-\gamma_T)\sum_r (W_i W_r)^{1/2} \times [B^c_{i,r}\cos(\varphi_i-\varphi_r) - B^s_{i,r}\sin(\varphi_i-\varphi_r)]\,,$$

$$\Delta\varphi_i = -\omega_i\delta T + \tfrac{1}{2}A\sum_r (W_r/W_i)^{1/2} \times [B^s_{i,r}\cos(\varphi_i-\varphi_r) + B^c_{i,r}\sin(\varphi_i-\varphi_r)]\,, \tag{1}$$

where

$$\delta T = T_c - T_e\,,$$

$$A = 4\pi^2(2\lambda_0/\lambda_q)^{1/2} \times \frac{L_w\lambda_0}{\Sigma_L}\left(\frac{I}{I_0}\right)\frac{k^2}{(1+k^2)^{3/2}}\left(\frac{\Delta\omega}{\omega}\right)_0^{-2}\,, \tag{2}$$

(W_i, φ_i) stand, respectively, for the laser field energy density and phase, γ_T are the cavity losses and (T_c, T_e) are the cavity round trip and electron bunch–bunch time distance respectively. Furthermore λ_0 is the resonant wave-length, λ_q, L_w are the wiggler wave-length and length, Σ_L is the laser beam (l.b.).cross section, I, I_0 are the average electron current and the Alfvén current respectively, k is proportional to the wiggler magnetic field, finally $(\Delta\omega/\omega)_0$ is the homogeneous bandwidth. (For further comments see refs. [2,3] and table 1).

Furthermore $B^{c,s}_{i,r}$ are given by

$$B^c_{i,r} = \mathrm{Re}\,B_{i,r}\,,\quad B^s_{i,r} = -\mathrm{Im}\,B_{i,r}\,, \tag{3}$$

and $B_{i,r}$ reads

$$B_{i,r} = \int f(z,\epsilon,a)\exp(\mathrm{j}(k_i-k_r)z) \times E\left(\nu_i + \mu_\epsilon\frac{\epsilon}{\sigma_\epsilon} - \mu_a\frac{a}{\sigma_a}, \nu_r + \mu_\epsilon\frac{\epsilon}{\sigma_\epsilon} - \mu_a\frac{a}{\sigma_a}\right)\mathrm{d}z\,\mathrm{d}\epsilon\,\mathrm{d}a. \tag{4}$$

The function $f(z, \epsilon, a)$ accounts for the electron beam (e.b.) distribution along the longitudinal direction, in energy and in emittance [4]; furthermore μ_ϵ and μ_a are the ratios between the *inhomogeneous widths* due to the energy spread and emittance of the electron beam and the homogeneous one [4], ν_i is proportional to the shift between the ith mode frequency ω_i and the resonant one ω_0; finally $E(\nu, \nu_0)$ can be written as (see refs. [2,3])

$$E(\nu, \nu_0) = \exp(\mathrm{j}\nu) \left\{ \frac{1}{\nu - \nu_0} \times \left[\frac{1-\exp(-\mathrm{j}\nu_0)}{\nu_0^2} - \frac{1-\exp(-\mathrm{j}\nu)}{\nu^2} \right] - \frac{\mathrm{j}}{\nu\nu_0} \right\} \tag{5}$$

Up to now the problem has been discussed in terms of the modal expansion introduced in ref. [2], which revealed itself useful in treating the small signal regime [2,3]. We have, however, to underline that, being the number of modes involved very high (10^3–10^4), such an expansion becomes unpleasing for an appealing physical description, and more and more cumbersome (although feasible) for further mathematical handling.

Let us therefore introduce a new expansion in terms of what we call supermodes (S.M.) which can be properly defined for the FEL operation. This expansion is not only mathematically simpler but allows, also, a simpler analysis of the interaction process. In fact the main physical features of the pulse propagation, lethargy and so on, are better clarified and explained.

We define an S.M. as the configuration of spatial modes, which reproduces itself after one passage throughout the interaction region. Therefore the equations which must obey the spatial modes (belonging to one S.M.) are [‡1]

$$\Delta W_i = \alpha W_i, \quad \Delta\varphi_i = \Psi, \tag{6}$$

where α and Ψ are identical for all the modes and are defined as gain and advance in phase per pass respectively.

The eq. (6) can be rehandled and comprised in a single one by using the following complex notation, already introduced in ref. [3].

$$x = (W)^{1/2} \exp(\mathrm{j}\varphi). \tag{7}$$

From (7) and (1) and a few algebra it follows that the eqs. (6) reduce to the following one

$$\hat{K}(\Theta; \mu_\mathrm{L}, \mu_\mathrm{c}, \mu_\epsilon, \mu_\mathrm{a})\boldsymbol{x} = q_\gamma \boldsymbol{x}, \tag{8}$$

[‡1] The above considerations are due to a discussion of the authors with A. Bambini.

where $\boldsymbol{x}$ is a column vector and

$$q_\gamma = \frac{1}{g_0}\left[\frac{\alpha+\gamma_\mathrm{T}}{1-\gamma_\mathrm{T}} + 2\mathrm{j}(\Psi + \omega_0\delta t)\right],$$
$$\hat{K}_{i,r} = -\left\{(2\pi)^{3/2}\frac{\mu_\mathrm{L}}{\mu_\mathrm{c}} B_{i,r} + \mathrm{j}\Theta\delta_{i,r}\nu_r\right\}, \tag{9}$$

g_0 and μ_L have been defined in table 1 and μ_c is the so called *coupling-width* [3].

The S.M. are the eigenstates of eq. (8). Namely the rth eigenvalue is the solution of the secular equation

$$\det(\hat{K} - \hat{\mathbf{1}}\, q_\gamma^r) = 0, \quad (\hat{\mathbf{1}} \equiv \text{Unity matrix}). \tag{10}$$

Let us notice that the spectrum of the eigenvalues of the eq. (10) is overcomplete as follows from the fact that $\hat{K}$ is not an hermitian operator but a *normal* one ($\hat{K}^\dagger\hat{K} = \hat{K}\hat{K}^\dagger$) (see e.g. ref. [5]), anyway we can always restrict our analysis to a subspace where we can define a complete base of eigenvalues.

The gain per pass relative to the eigenstate r can be obtained from the first of eqs. (9) and reads

$$\alpha^r = g_0(1-\gamma_\mathrm{T})\,\mathrm{Re}\, q_\gamma^r - \gamma_\mathrm{T}. \tag{11}$$

Before discussing the numerical analysis of eq. (8) let us rewrite it in a form which has a more appealing physical meaning. It comes out to be expedient to understand eq. (8) in terms of a quantity linked to the laser electric field rather than to the longitudinal cavity modes. To this aim we define [3]

$$\zeta(s) = \sum_i x_i \exp\left(\mathrm{j}\frac{\nu_i}{\mu_\mathrm{L}}\frac{s}{L_\mathrm{c}}\right), \quad (|s| \leqslant L_\mathrm{c}/2). \tag{12}$$

Recalling that the laser field is circularly polarized, it is easily understood that $\zeta(s)$ is proportional to $E_x + \mathrm{j}E_y$ ($E_{x,y}$ being the electric field transverse components). Furthermore the laser power density profile, owing to (12), reads

$$\mathrm{d}P_\mathrm{L}/\mathrm{d}S = c\,|\zeta(s)|^2. \tag{13}$$

By inverting the eq. (12), each x_i can be expressed in terms of $\zeta(s)$ as

$$x_i = \frac{1}{L_\mathrm{c}}\int_{-L_\mathrm{c}/2}^{+L_\mathrm{c}/2} \zeta(s)\exp\left(-\mathrm{j}\frac{\nu_i}{\mu_\mathrm{L}}\frac{s}{L_\mathrm{c}}\right)\mathrm{d}s, \tag{14}$$

where $\nu_i = 2\pi n_i \mu_\mathrm{L}$ and n_i is an integer.

Eq. (8) can be now rewritten by means of (14) as follows [‡2]

$$q_\gamma \zeta(s) + \Theta\Delta\, \mathrm{d}\zeta(s)/\mathrm{d}s = -\mathrm{j}\,[(2\pi)^{3/2}/\mu_c\Delta^2] \times \int_0^\Delta y\,\mathrm{d}y\, \zeta(s+y)\, \frac{\exp(-\mu_\epsilon^2 y^2/2\Delta^2)}{1+\mathrm{j}\mu_a y/\Delta} \int_{s+y}^{s+\Delta} f(z)\,\mathrm{d}z\,, \tag{15}$$

where Δ is the maximum e.b.–l.b. slippage due to the different velocity between electrons and photons (for further comments see ref. [3]).

In deducing eq. (15) it has been used the following periodicity condition

$$\zeta(-L_c/2) = \zeta(L_c/2); \tag{16}$$

furthermore the e.b. distribution function has been assumed to have the following form

$$f(z,\epsilon,a) = (1/\sqrt{2\pi}\,\sigma_\epsilon\sigma_a) \times \exp\{-[\epsilon^2/2\sigma_\epsilon^2 + a/\sigma_a]\}\cdot f_0(z)\,, \tag{17}$$

$(-L_c/2 \leqslant z \leqslant L_c/2)$.

The physical meaning of eq. (15) is transparent: the *electric-field* $\zeta(s)$ depends on the assumed value at $s+y$, where y varies from 0 to maximum e.b.–l.b. slippage Δ.

Numerical results

Eq. (15) is very general and can be specialized to the following interesting case ‡3

(a) *Homogeneously broadened emission line [4]*

$$\mu_\epsilon \ll 1\,, \quad \mu_a \ll 1\,, \tag{18}$$

(b) *Short e.b.* ($\sigma_z \equiv$ r.m.s. e.b. length)

$$\sigma_z \ll L_c \Rightarrow \mu_c \gg \mu_L\,. \tag{19}$$

(c) *Continuous spectrum approximation* (refs. [3,4])

$$\mu_L \ll 1\,. \tag{20}$$

In this connection eq. (15) is significantly simplified and its eigenvalues are functions of the parameters Θ and μ_c.

‡2 Let us stress that eq. (15) is an integro-differential equation fully equivalent to the linear algebraic equation (8). Thus its solutions give the field amplitudes which reproduce itself after a passage throughout the wiggler.

‡3 It is to be noticed that such conditions are the operating ones for the Stanford experiment, in addition condition (a) is peculiar for the Stanford machine, while (b) and (c) are general operating conditions for single pass machines (e.g. Linac or microtron).

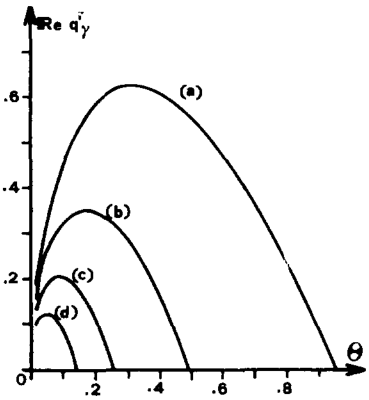

Fig. 1. Re q^r_γ versus Θ for the first four eigenstates (μ_c = 1.0). (a) r = 1, (b) r = 2, (c) r = 3, (d) r = 4.

As example we have plotted in fig. 1 Re q^r_γ (r = 1, ..., 4; Re $q^{r+1}_\gamma <$ Re q^r_γ) versus Θ at $\mu_c = 1$.

We have to stress that we have positive values of Re q^r_γ for $\Theta > 0$; thus being Θ linked to $-\delta T$ we must require that the optical cavity round trip must be shorter than the time distance between two adjacent electron bunches. This effect is linked to the FEL *lethargy*, already discussed in refs. [3,6].

In fig. 2 have been reported Re q^1_γ and $\bar{\tau}$ defined as

$$\bar{\tau} = \bar{s}/\sigma_z\,, \tag{21}$$

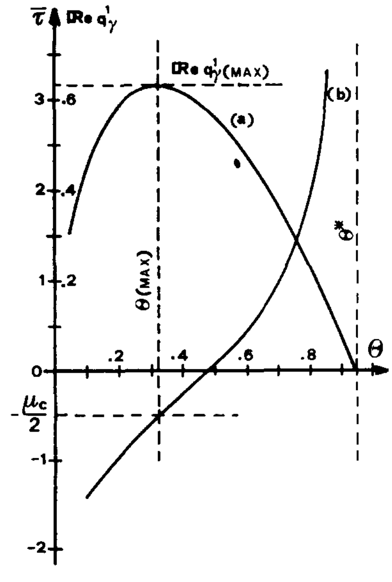

Fig. 2. Curve (a): Re q^1_γ versus Θ (μ_c = 1.0). Curve (b): $\bar{\tau}$ versus Θ (μ_c = 1.0).

where $\bar{s}$ is the shift between the l.b. and e.b. at the interaction starting time, which reads

$$\bar{s} = \int s|\zeta(s)|^2\,ds \Big/ \int |\zeta(s)|^2\,ds\,. \tag{22}$$

From the figure it appears that the maximum of $\mathrm{Re}\,q_\gamma^1$ corresponds to $-\mu_c/2$. This can be understood if one notices that the difference between the l.b. and e.b. velocity is such that after one wiggler passage the vacuum phase slippage is given by $\Delta = \mu_c\sigma_z$ (see e.g. ref. [3]). This implies that the maximum of $\mathrm{Re}\,q_\gamma^1$ must correspond to the average shift for which the l.b. would explore, during the interaction, the most *conspicuous* part of the e.b. Such a shift, assuming a gaussian distributed e.b., is $-\mu_c\sigma_z/2$.

In fig. 3 have been reported Θ versus $\mathrm{Re}\,q_\gamma^1$ for different values of μ_c. It is to be noticed that for increasing μ_c we have decreasing eigenvalues. This is a not surprising behaviour, indeed to large values of the μ_c parameter corresponds an e.b. length small with respect to the vacuum phase slippage Δ (see table 1).

Let us introduce the Fourier transform of $\zeta(s)$, which in the continuous spectrum approximation ($\mu_L \to 0$) reads (see eq. (14))

$$x(\nu) = \frac{1}{2\pi\mu_c\sigma_z}\int_{-\infty}^{+\infty} \zeta(s)\exp(-j\nu s/\mu_c\sigma_z)\,ds\,. \tag{23}$$

In figs. 4, 5 we have reported $|x(\nu)|^2$ and $|\zeta(s)|^2$ respectively, for the eigenvalue $r = 1$ at $\mu_c = 1$, for different values of Θ (0.1, 0.4, 0.7). The curve (α) in fig. (4) re-

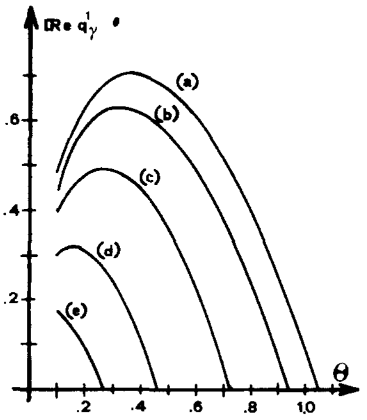

Fig. 3. $\mathrm{Re}\,q_\gamma^1$ versus Θ. (a) $\mu_c = 0.5$, (b) $\mu_c = 1.0$, (c) $\mu_c = 2.0$, (d) $\mu_c = 4.0$, (e) $\mu_c = 8.0$.

Table 1
We summarize in the following table the main notations used throughout the text, a complete discussion of the meaning of the symbols can be found in refs. [2,3,4]

1.1. *Wiggler parameters*

λ_q	$\equiv$ Wiggler wave-length
L_W	$\equiv$ Wiggler length
B_0	$\equiv$ Wiggler peak magnetic field
k	$= (e/2\pi)B_0\lambda_q/m_0c^2$

1.2. *Optical cavity parameters*

L_c	= Optical cavity length
T_c	$= L_c/c \equiv$ (Optical cavity round trip period)
ω_i	$= 2\pi n_i/T_c \equiv$ (frequency of the ith longitudinal eigenmode, n_i integer)
k_i	$= \omega_i/c$
γ_T	$\equiv$ Optical cavity losses.

1.3. *Electron beam parameters*

ϵ	$\equiv$ Electron energy
σ_ϵ	$\equiv$ r.m.s. relative energy spread
σ_z	$\equiv$ r.m.s. bunch length
a	$\equiv$ Electron emittance
σ_a	$\equiv$ r.ms.. emittance
N_e	$\equiv$ number of electrons per bunch
T_e	$\equiv$ Time distance between two adjacent bunches
I	$= N_e e/T_e \equiv$ average electron current
I_p	$= cT_e I/\sqrt{2\pi}\,\sigma_z$
I_0	$= ec/r_0 \equiv$ Alfvén current

1.4. *Laser beam parameters*

λ_0	$= (\lambda_q/2)(1+k^2)(m_0c^2/E_0)^2 \equiv$ resonant wave-length
ω_0	$= 2\pi c/\lambda_0$
W_i, φ_i	$\equiv$ Energy density and phase of the ith laser mode
$(\Delta\omega/\omega)_0$	$= \lambda_q/2L_W \equiv$ homogeneous bandwidth
$(\Delta\omega/\omega)_\epsilon$	$= 2\sigma_\epsilon \equiv$ inhomogeneous bandwidth (energy-spread)
$(\Delta\omega/\omega)_a$	$= (\sqrt{2}k/\sqrt{1+k^2})\,\sigma_a/\sqrt{\lambda_0\lambda_q} \equiv$ inhomogeneous bandwidth (emittance) [4]
μ_ϵ	$= (\Delta\omega/\omega)_\epsilon/(\Delta\omega/\omega)_0$
μ_a	$= (\Delta\omega/\omega)_a/(\Delta\omega/\omega)_0$
$(\Delta\omega/\omega)_c$	$= \lambda_0/2\sigma_z \equiv$ coupling width
μ_c	$= (\Delta\omega/\omega)_c/(\Delta\omega/\omega)_0$
Δ	$= \mu_c\sigma_z \equiv$ vacuum phase slippage
δT	$= T_c - T_e$
Θ	$= -(2/\pi)(\Delta\omega/\omega)_0\,\omega_0\delta t/g_0$
$\dfrac{\omega_{i+1}-\omega_i}{\omega_0}$	$= \lambda_0/L_c$
μ_L	$= (\lambda_0/2L_c)/(\Delta\omega/\omega)_0$
ν_i	$= \pi(\Delta\omega/\omega)_0^{-1}(\omega_0-\omega_i)/\omega_0$
Σ_L	$\equiv$ Laser beam cross section
g_0	$= 2\pi\left(\dfrac{2\lambda_0}{\lambda_q}\right)^{1/2}\left(\dfrac{I_p}{I_0}\right)\left(\dfrac{L_W\lambda_0}{\Sigma_L}\right)\dfrac{k^2}{(1+k^2)^{3/2}}\left(\dfrac{\Delta\omega}{\omega}\right)_0^{-2}$

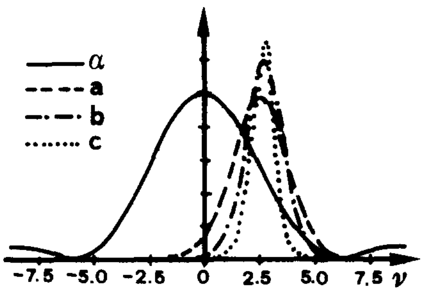

Fig. 4. Spectrum relative to the first eigenstate for $\mu_c = 1.0$ (a) $\Theta = 0.1$, (b) $\Theta = 0.4$, (c) $\Theta = 0.7$. (α) spontaneous emission spectrum.

fers to the spontaneus emission spectrum [2], while that in fig. 5 to the e.b. longitudinal distribution function. As it can be seen, for increasing Θ we have decreasing bandwidth (see fig. 4), while the l.b. is pushed ahead the e.b. and its length increases (see fig. 5).

In fig. 6 we report versus Θ at $\mu_c = 1$ the quantities σ_ν and σ_τ linked, respectively, to the laser bandwidth and length by

$$(\Delta\omega/\omega)_L = (1/\pi)(\Delta\omega/\omega)_0\,\sigma_\nu\,,$$
$$\sigma_s = \sigma_z \cdot \sigma_\tau\,. \tag{24}$$

From fig. 6, too, one can see that with increasing Θ the laser bandwidth decreases and the l.b. length increases (compare this with figs. 4, 5).

In figs. 7, 8 have been reported $|x^r(\nu)|^2$ and $|\zeta^r(s)|^2$ at fixed $\Theta = 0.2$ and $\mu_c = 1$ ($r = 1, 2, 3$). It can be noticed that once the order of the eigenvalue increases $|\zeta^r(s)|^2$ shows an increasing number of peaks, so that

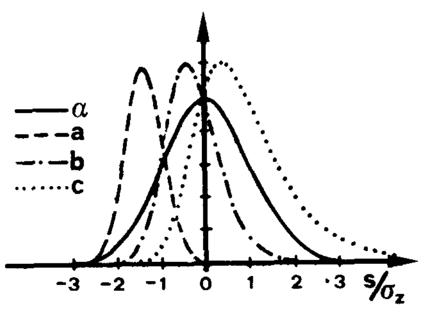

Fig. 5. Power density profile relative to the first eigenstate for $\mu_c = 1.0$. (a) $\Theta = 0.1$, (b) $\Theta = 0.4$, (c) $\Theta = 0.7$. (α) electron beam density profile.

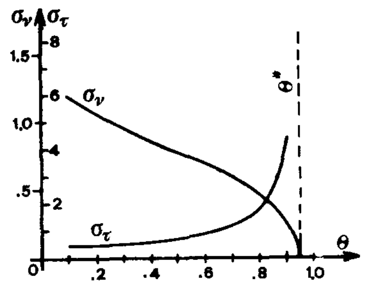

Fig. 6. Curve (a): σ_ν versus Θ ($\mu_c = 1.0$, first eigenstate). Curve (b): σ_τ versus Θ ($\mu_c = 1.0$, first eigenstate).

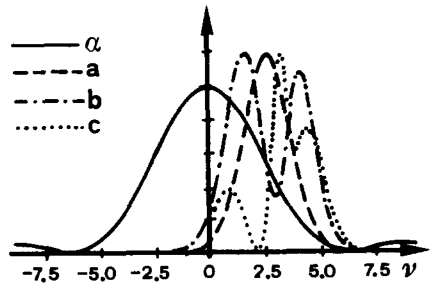

Fig. 7. Spectrum relative to the first three eigenstates for $\mu_c = 1.0$. (a) $r = 1$, (b) $r = 2$, (c) $r = 3$. (α) spontaneous emission spectrum.

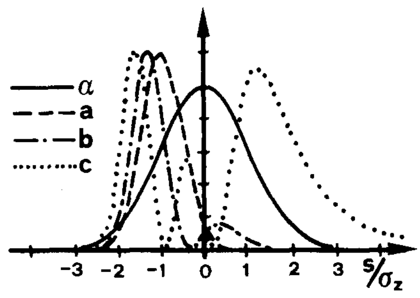

Fig. 8. Power density profile relative to the first three eigenstates for $\mu_c = 1.0$. (a) $r = 1$, (b) $r = 2$, (c) $r = 3$. (α) electron beam density profile.

more and more sidebands appear in the laser spectrum $|x^r(\nu)|^2$.

Let us now go back to fig. 1 for some final remarks. Recalling that $\mathrm{Re}\,q_\gamma^r$ is linked to the gain per pass by the eq. (11), it is easily understood that once are fixed both a particular value of Θ and the cavity losses one can settle out the eigenvalues which play no role. Furthermore one expects that the eigenstates above threshold would interfere and thus the resulting spectrum would exhibit a number of peaks. A correct analysis of this interfering needs the knowledge of the amount of the contribution of each eigenvalue to the spectrum. Anyway the knowledge of such contributions requires a strong signal analysis which will be considered elsewhere.

In addition one can define an operating region for Θ which in turn fixes the maximum cavity length variation for the laser operation and the upper limit for the strong signal operation. Using the characteristics of the Stanford apparatus [7], from our picture it follows that the maximum cavity length variation ranges from 20 to 10 μm for $\mu_c = 1, 2$ respectively, the Stanford experimental data was 5 μm. It is to be recalled however that our small signal analysis gives only an upper limit and that there is some uncertainty in defining μ_c owing to the lack of precise knowledge about the σ_z of the Stanford e.b.

The authors greatly express their gratitude to A. Bambini for his continuous assistance during the compilation of the paper, for enlightening comments and discussions and for a careful analysis of the manuscript.

References

[1] L.R. Elias, W.M. Fairbank, J.M.J. Madey, H.A. Schwettman and T.I. Smith, Phys. Rev. Lett. 36 (1976) 717; D.A.G. Deacon, L.R. Elias, J.M.J. Madey, G.J. Ramian, H.A. Schwettman and T.I. Smith, Phys. Rev. Lett. 38 (1977) 892.

[2] G. Dattoli and A. Renieri, Lett. Nuovo Cimento 24 (1979) 121; Nuovo Cimento B59 (1980) 1. G. Dattoli and A. Renieri, CNEN Report 79.37/p, Centro di Frascati, Frascati, Rome, Italy.

[3] G. Dattoli and A. Renieri, Nuovo Cimento B 59 (1980) 1.

[4] A. Renieri, CNEN Report 78.9/cc, Centro di Frascati, Frascati, Rome, Italy; Lectures given at the LXXIV International School of Physics Enrico Fermi, 2nd Course 1978 Development in High power lasers and their applications, Varenna, July 1978, to appear in the proceedings of the School.

[5] M. Reed and B. Simmons, Methods of modern mathematical physics, Vol. IV, Analysis of operators (Academic Press, New York 1978).

[6] H. Al-Abawi, F.A. Hopf, G.T. Moore and M.O. Scully, Optics Comm. 30 (1979) 235.

[7] H.A. Schwettman and J.M.J. Madey, final technical report to ERDA (1977), High Energy Physics Laboratory, Stanford University, Stanford, California.